

Electronic Supplementary Information

A facile reflux method for in situ fabrication of non-cytotoxic $\text{Bi}_2\text{S}_3/\beta\text{-Bi}_2\text{O}_3/\text{ZnIn}_2\text{S}_4$ ternary photocatalyst: A novel dual Z-scheme system with enhanced multifunctional photocatalytic Activity

Dibyananda Majhi^a, Krishnendu Das^a, Ranjit Bariki^a, Subash Padhan^b, Abtar Mishra^c, Rohan Dhiman^c, Priyanka Dash^c, Bismita Nayak^c, B.G. Mishra^{a*}

^a*Department of Chemistry, National Institute of Technology, Rourkela-769008, Odisha, India*

^b*Department of Applied Chemistry, IIT Dhanbad, Jharkhand-826004*

^c*Department of Life Science, National Institute of Technology, Rourkela-769008, Odisha, India*

*Corresponding author

B.G. Mishra

Email: brajam@nitrkl.ac.in

Synthesis of β -Bi₂O₃. The tetragonal phase of Bi₂O₃ (β -Bi₂O₃) was synthesized by using our previously reported method.¹ In this procedure, initially tetragonal Bi₂O₂CO₃ was prepared by hydrothermal method (160°C for 24 h) taking Bi(NO₃)₃·5H₂O, Urea and KBr (1:5:1 molar ratio). The as prepared Bi₂O₂CO₃ material is then calcined at 400°C for 3 h to get tetragonal phase of Bi₂O₃. The material obtained is named as BO.

Synthesis of ZnIn₂S₄. In a typical synthesis procedure, Zn(NO₃)₂·6H₂O, InCl₃ and thioacetamide (TAA) were taken in 1:2:4 molar ratios. The schematic illustration to prepare the material is depicted below in Figure S1. The prepared material is labeled as ZIS in the manuscript.

Synthesis of Bi₂S₃. For synthesis of Bi₂S₃, Bi(NO₃)₃·5H₂O and thioacetamide (1:5 molar ratio) were dissolved in 60 ml distilled water in a round bottom flask by repeated sonication and stirring for 30 min. Then the resultant solution was refluxed for 3 h under continuous stirring condition. The resultant solid residue was washed with water and ethanol several times and then subjected to vacuum drying for 12 h. The as synthesized material is named as BS.

Synthesis of ZnIn₂S₄/β-Bi₂O₃ (ZIS/BO) and Bi₂S₃/ZnIn₂S₄ (BS/ZIS) composite materials. A rational self-assembly approach was adopted to synthesize the binary ZnIn₂S₄/β-Bi₂O₃ and Bi₂S₃/ZnIn₂S₄ composite materials. In a typical synthesis procedure to prepare ZnIn₂S₄/β-Bi₂O₃, a certain amount of β-Bi₂O₃ (200 mg) was added into 30 mL of methanol with continuous stirring for 30 min. Subsequently, as synthesized ZnIn₂S₄ (20 wt%) was added to the above solid suspension and kept under continuous stirring condition for 2 h. After the methanol was evaporated, the solid product obtained was subjected to vacuum drying for 12 h. The resulting sample was named as ZIS/BO in the manuscript. The ZnIn₂S₄ material is also hybridized with 20 wt% of Bi₂S₃ using similar procedure. The obtained binary Bi₂S₃/ZnIn₂S₄ composite was labeled as BS/ZIS in the manuscript.

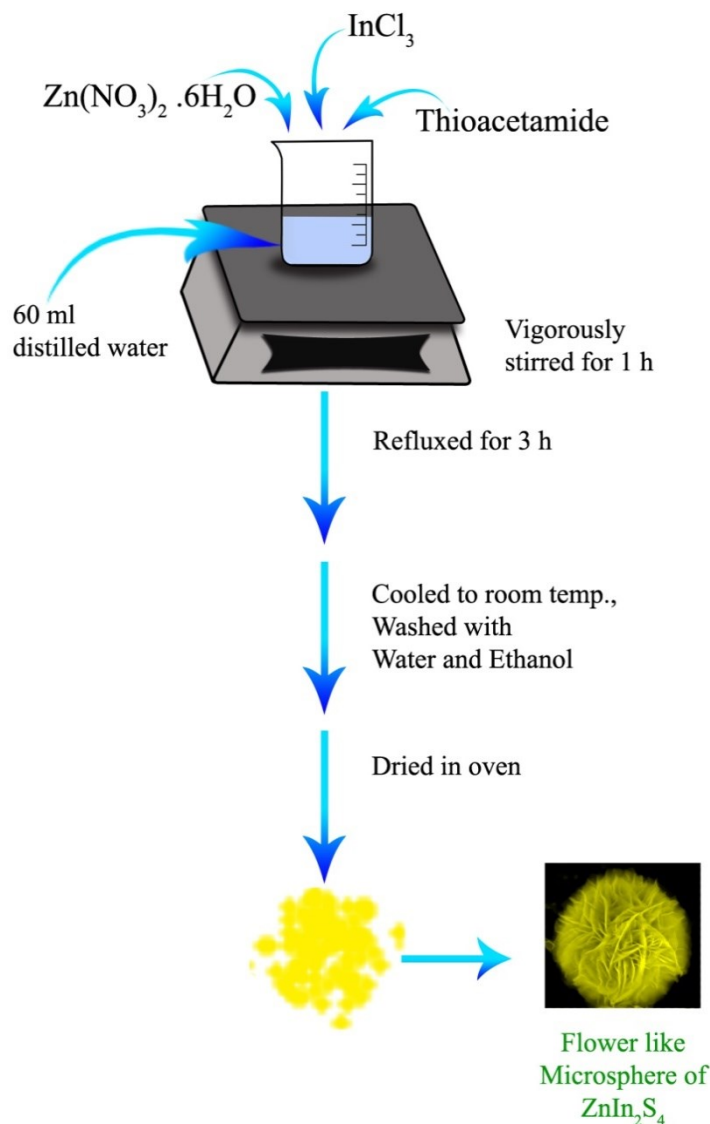


Fig. S1 Schematic illustration for facile reflux synthesis of ZnIn₂S₄.

Characterization Techniques. The phase identification of prepared photocatalysts was performed using a Rigaku Ultima-IV X-ray diffractometer fitted with CuK α radiation ($\lambda = 1.5418 \text{ \AA}$) as X-ray source. The UV-Vis diffuse reflectance spectra of all the samples were recorded using a Jasco V-650 spectrometer. The stretching and bending vibration modes of the functional groups present in the materials were characterized by a Perkin–Elmer infrared spectrometer using KBr as reference matrix. Raman analysis was carried out using a WITec alpha 300R spectrometer. The morphological and microstructural properties were acquired using FESEM (Nova Nano SEM/FEI microscope) and TEM (TECNAI 300 kV instrument) techniques, respectively. The

photoluminescence (PL) spectra and three-dimensional excitation–emission fluorescence spectra (3D-EEMs) were recorded using a Horiba Scientific Fluoromax-4 spectrometer. X-ray photoelectron spectroscopy measurements were performed using a SPECS spectrophotometer (Germany). The fluorescence life time measurements were carried out using Edinburgh Spectrofluorometer FS-5 instruments with SC-10 and SC-30 integrating sphere module. ESR analysis was carried out to determine the formation of hydroxyl and superoxide radicals in the aqueous and methanolic suspension of the ternary composite photocatalyst using a Bruker ELEXSYS 550 X band EPR spectrometer. LC-ESI-MS analysis was performed to identify the intermediates/degradation products during the photocatalytic degradation of TCN (Perkin-Elmer, Flexar SQ 300). The mobile phase consists of a mixture of acetonitrile and formic acid (0.1%) with a flow rate 0.10 mL min^{-1} . An injection volume of $10 \text{ }\mu\text{L}$ and a C18 column ($2.1 \text{ mm} \times 100 \text{ mm}$, $1.7 \text{ }\mu\text{m}$, 30°C) was used for LC-ESI-MS study.

Photoelectrochemical Measurements. All the photoelectrochemical characterizations were carried out in a CHI660C electrochemical workstation having a standard three electrode system. Prior to the measurements, samples were well dispersed in isopropyl alcohol and a thin film (1 cm^2 sample area) was prepared over FTO substrate which serves as a working electrode. Platinum wire was used as counter electrode whereas Ag/AgCl serves as the reference electrode. The impedance measurements were conducted in the frequency range of 100 kHz to 10 mHz with 10 mV magnitude of modulation. Photocurrent response was recorded *w.r.t.* time in presence and absence of light with approximately 30 s time interval of light on and off mode. Linear sweep voltammetry measurements were performed in the range of $0\text{-}1.5 \text{ V}$ at a scan rate of 10 mVs^{-1} . Further, the Mott-Schottky measurements were carried out at 1 kHz frequency. The measurements were performed at room temperature by taking $0.1 \text{ M Na}_2\text{SO}_4$ as supporting electrolyte.

Photocatalytic Activity Test.

Tetracycline Degradation. For this degradation study, initially 100 ppm stock solution of TCN was prepared. In each photocatalytic experiments, 30 mg of photocatalyst was well dispersed in 100 ml (20 ppm) TCN solution by ultra-sonication. Prior to the light irradiation, the aqueous suspension was stirred for 30 min under dark condition to achieve adsorption-desorption equilibrium. The photocatalytic reaction was carried out using an immersion well quartz photoreactor fitted with a 250 W Xe lamp ($\lambda > 420 \text{ nm}$). The light intensity at the external surface of the reactor was found to be 45.4 mW/cm^2 . After light irradiation, 3 ml of sample was collected

at given time interval and centrifuged. The supernatant solution was analyzed at absorption wavelength of 357 nm using a Jasco V-650 UV-Vis spectrometer. The photodegradation efficiency (PDE) (%) was calculated using the following formula.

$$PDE(\%) = \frac{A_0 - A_t}{A_0} \times 100 \dots\dots\dots(1)$$

Where A_0 and A_t represents the absorbance of TCN solution at 0 min (after adsorption) and different time interval of photocatalytic reaction, respectively.

Cr(VI) Reduction. To study the photoreduction of Cr(VI) to Cr(III), 30 mg photocatalyst was added to 100 mL Cr(VI) solution (10 mg L^{-1}) containing 4 mmol tartaric acid. The pH of the aqueous suspension was maintained at 2.0 using 2 M H_2SO_4 solution. The mixture was placed in dark condition under constant stirring for 30 min to attain adsorption-desorption equilibrium before being exposed to visible light. At regular time interval, 3 mL aliquots was withdrawn and centrifuged to separate the suspended solids. The concentration of Cr(VI) in the aqueous solution was determined at $\lambda = 540 \text{ nm}$ using diphenylcarbazide (0.25 wt% in acetone) (DPC) as complexing agent which forms violet color with Cr(VI).² The catalytic performance for Cr(VI) reduction was also assessed using different amount of tartaric acid as holes scavenger. The photoreduction efficiency (PRE) (%) was calculated using the following formula.

$$PRE(\%) = \frac{C_0 - C_t}{C_0} \times 100 \dots\dots\dots(2)$$

Where C_0 represents the initial Cr(VI) concentration after equilibrium experiment in dark and C_t is the Cr(VI) concentration after photoreduction process.

H₂ evolution. The photocatalytic activity of BZ20BO ternary heterostructure material was also studied for hydrogen evolution reaction using methanol as sacrificial agent. The hydrogen evolution reaction was performed using a pyrex glass photoreactor with a closed gas circulation system. In a typical experiment, 80 mg of the photocatalyst was dispersed in 80 ml (10 vol %) aqueous methanol solution by stirring for 30 min. The reactor was purged continuously with N_2 gas for 30 min to maintain an inert environment inside the photoreactor. The catalyst suspension was subsequently irradiated using a 250 W xenon lamp as visible light source. The photocatalytic H_2 evolution reaction was continued for 3h and the amount of H_2 gas evolved was measured by a

NUCON 5765 GC model fitted with a TCD detector at different time interval. For H₂ generation, the conversion efficiency for the hydrogen energy is calculated by using equation (3).

$$\text{Conversion efficiency (\%)} = \frac{\text{Stored chemical energy}}{\text{Energy of incident photon}} \times 100 \dots\dots\dots$$

.....(3)

Photocatalytic Bacterial Inactivation. The photocatalytic effect of BZ20BO against *Enterobacter cloacae* was studied using a standard protocol.³ Briefly, 5 µl of *Enterobacter cloacae* culture was inoculated in 5 ml Mueller Hinton Broth (MHB) which was then incubated at 37°C for 18 h under continuous shaking condition. After completion of the incubation period, the bacterial cells were harvested by centrifugation at 4000 rpm for 5 min. The supernatant was discarded and the obtained bacterial cell pellets were washed with 0.9% normal saline solution (NSS) for two times at same condition. The ternary BZ20BO material (300 mg/L concentration) was then suspended in the sterilized saline solution containing the cell pellets which was incubated for 1 h in dark. The catalyst solution was then exposed to visible light irradiation using Xenon lamp (250 W). At different time intervals, aliquots of the sample were then uniformly spread on sterilized Mueller Hinton Agar (MHA) plate which was further incubated overnight at 37°C. An agar plate spread only with the *Enterobacter* culture was considered as negative control. Light control plate was also prepared in which *Enterobacter* culture was exposed only to visible light irradiation without the photocatalyst. Similarly, photocatalyst nanoparticles together with the bacterial cells without light exposure were considered as dark control.

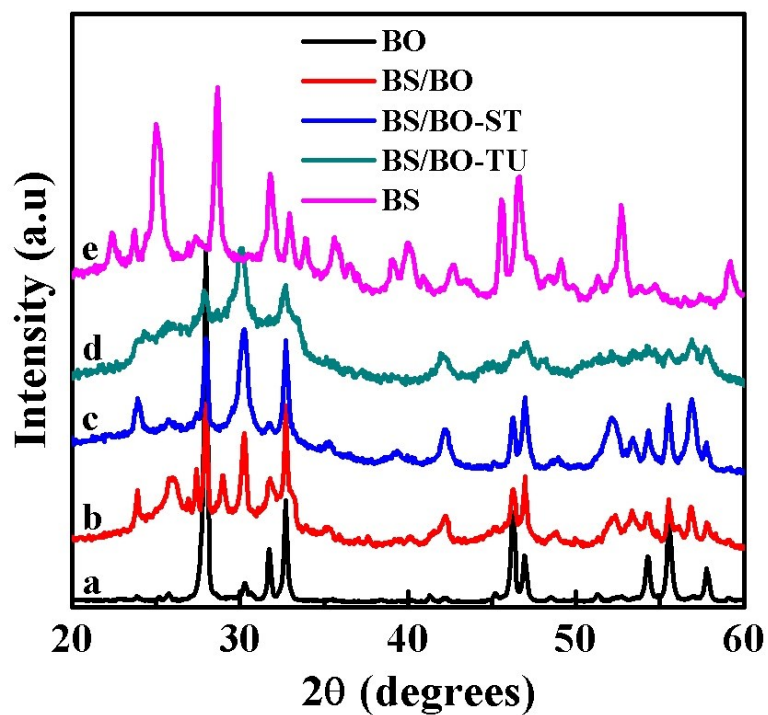


Fig. S2 XRD patterns of (a) BO, (b-d) BO treated with thioacetamide (BS/BO), sodium thiosulfate (BS/BO-ST) and thiourea (BS/BO-TU) respectively, under reflux condition and (e) BS sample.

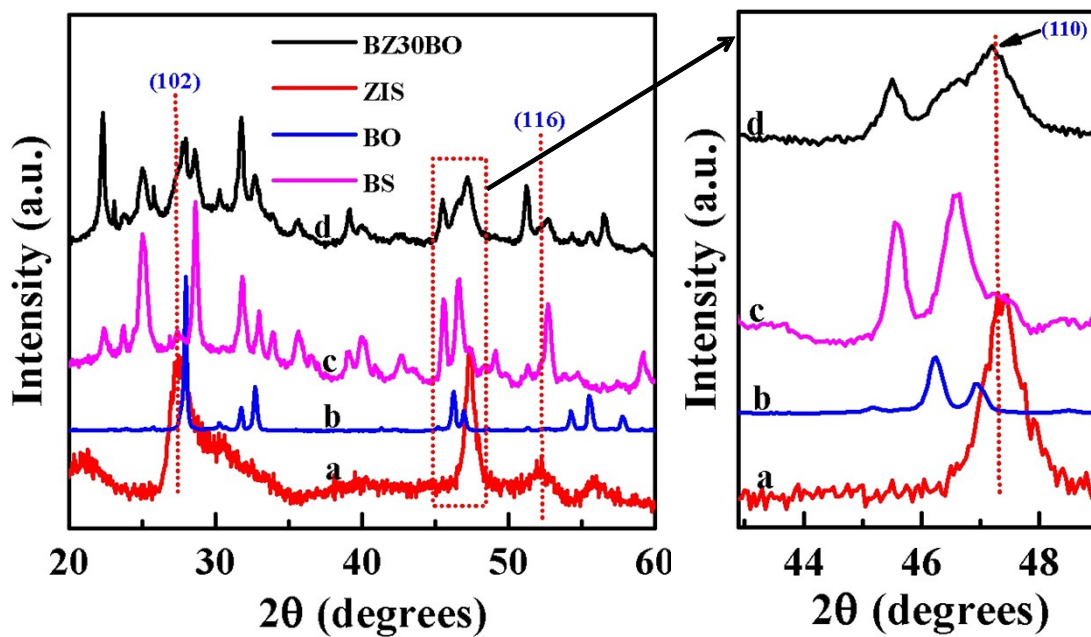


Fig. S3 XRD patterns of (a) ZIS, (b) BO, (c) BS and (d) BZ30BO samples.

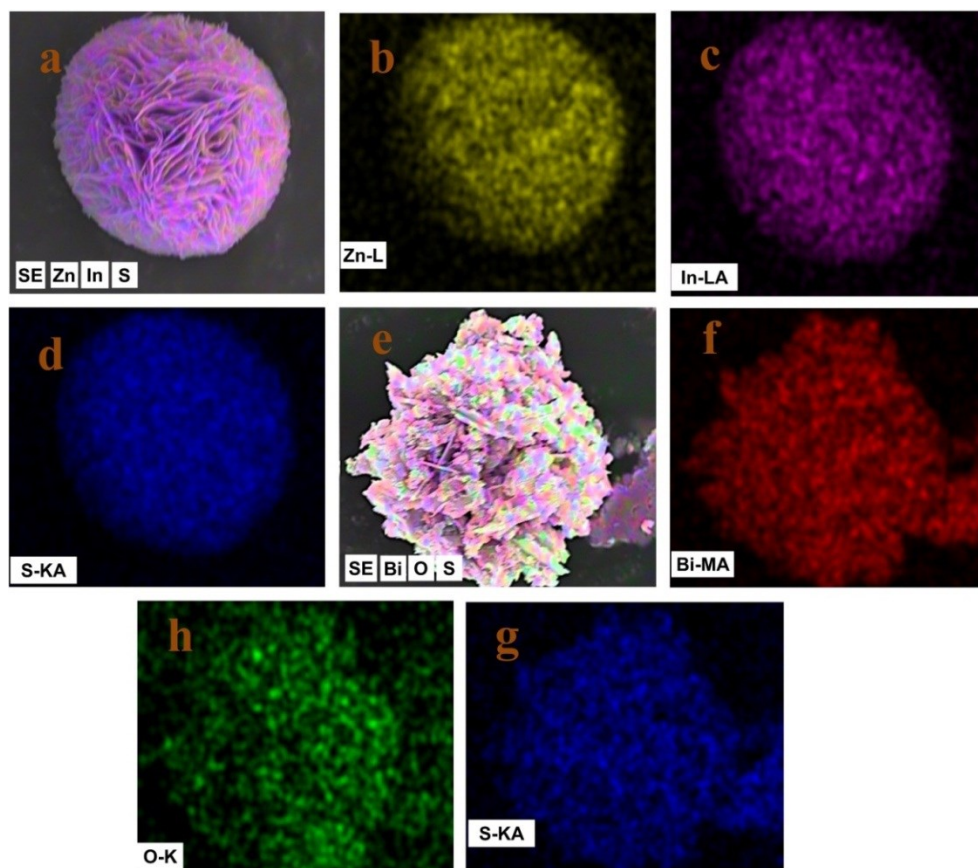


Fig. S4 Elemental mapping images of (a-d) ZIS and (e-g) BS/BO heterostructure materials.

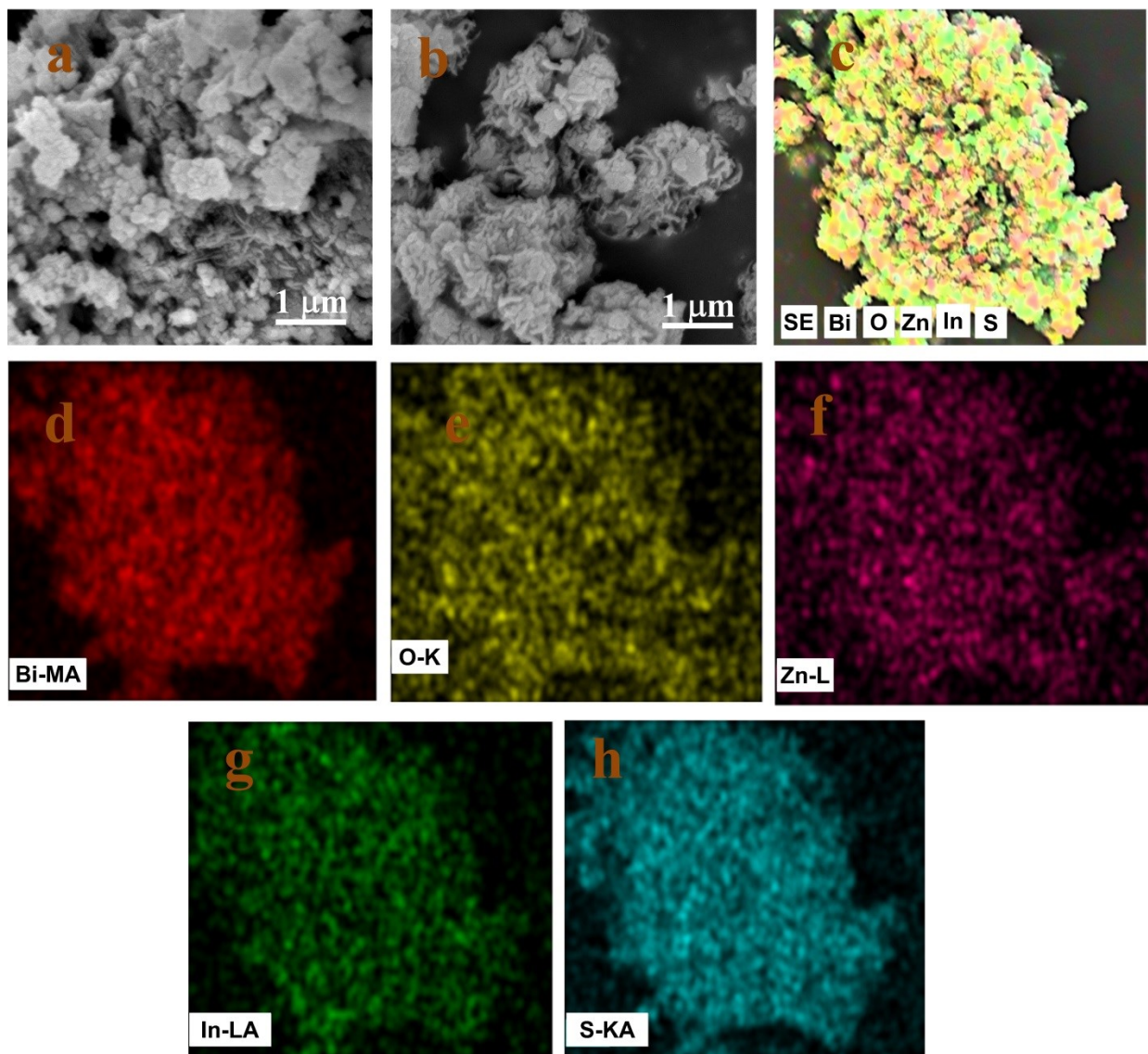


Fig. S5 FESEM images of (a) BZ5BO, (b) BZ10BO and Elemental mapping images of (c-h) BZ20BO ternary heterostructure materials.

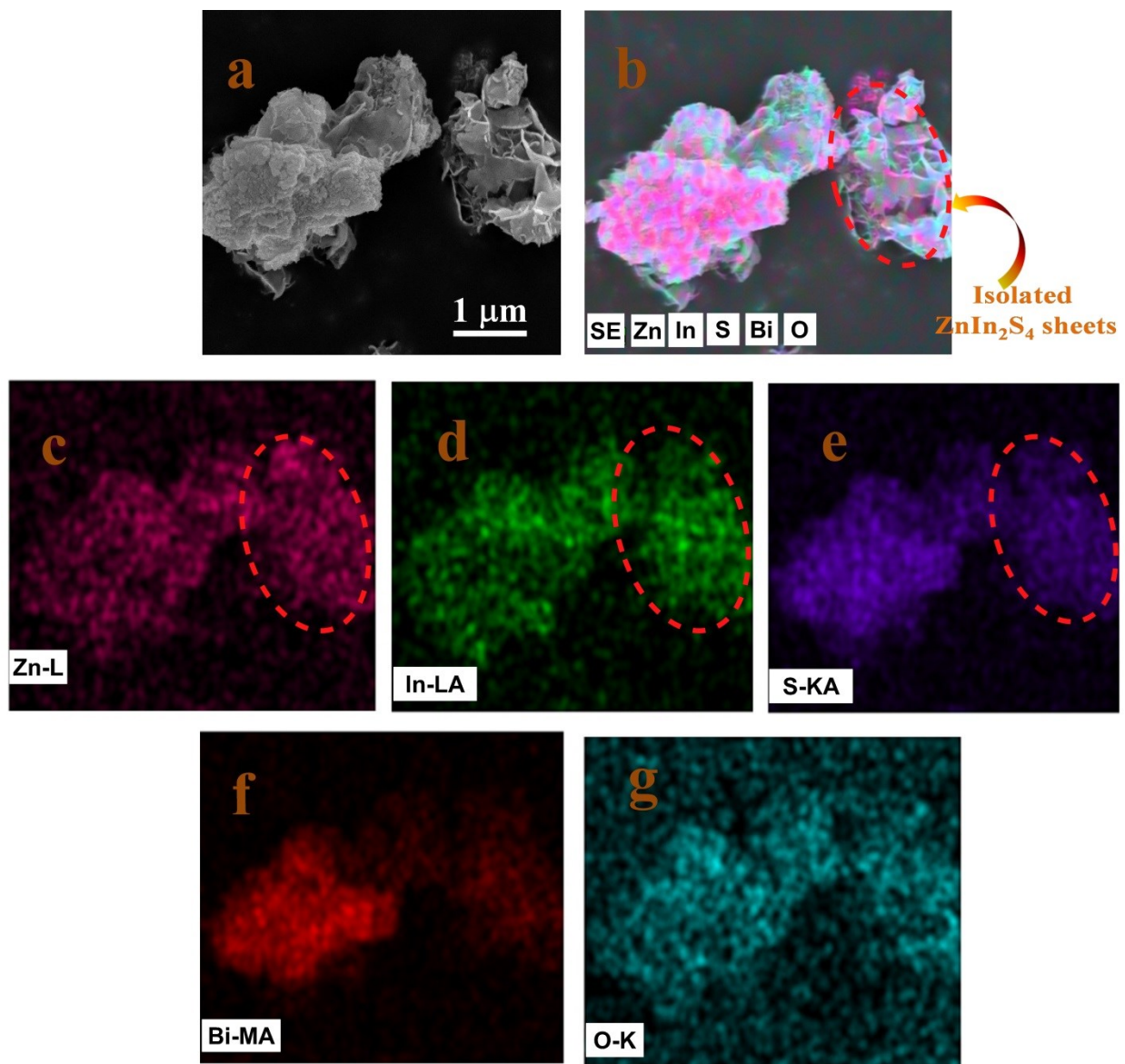


Fig. S6 (a) FESEM image and (b-g) elemental mapping images of BZ30BO material.

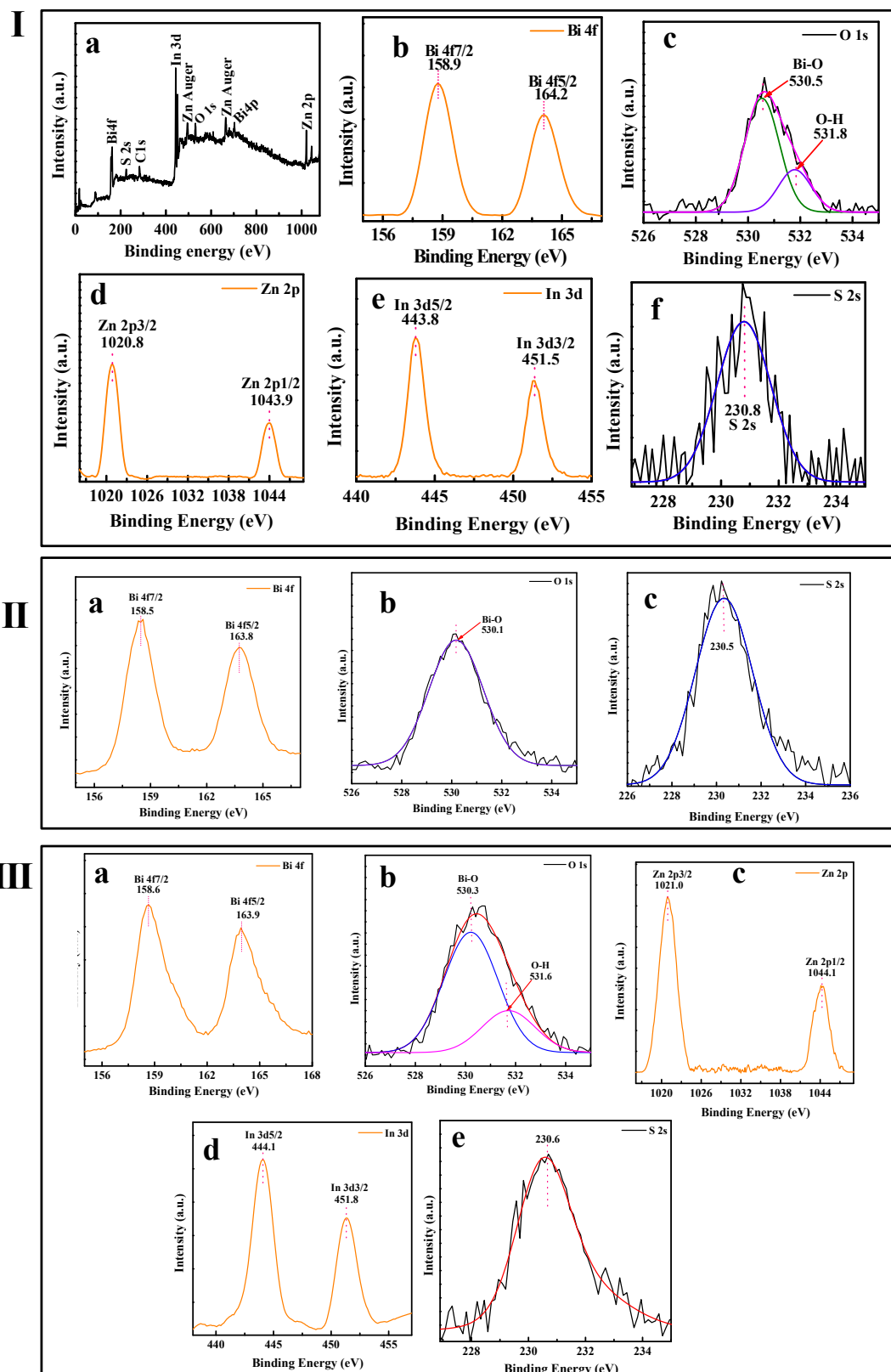


Fig. S7 XPS spectra of (I) BZ20BO, (II) BS/BO and (III) ZIS/BO materials.

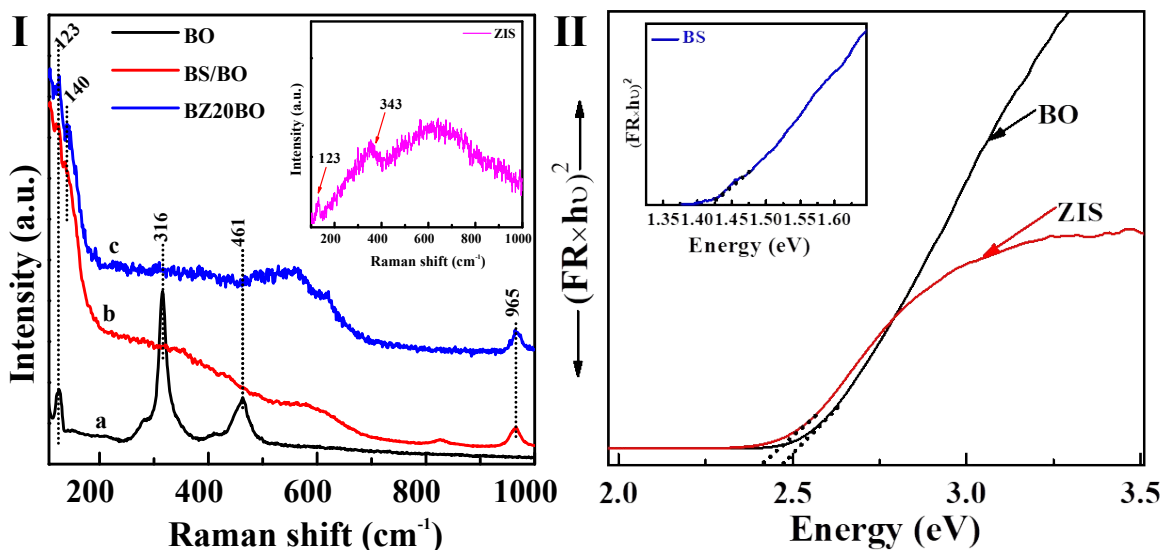


Fig. S8 (I) Raman spectra of (a) BO, (b) BS/BO and (c) BZ20BO and ZIS (Inset) and (II) Tauc's plot for the pure semiconductor materials.

Raman study:

The Raman spectra of pure BO, ZIS, binary BS/BO and ternary BZ20BO material is presented in Fig. S8I. Pure BO material exhibit Raman bands at 123, 316 and 461 cm⁻¹ which are characteristic of tetragonal β -Bi₂O₃ phase. Pure ZIS shows a broad Raman feature with peaks at 123 and 343 cm⁻¹. These bands are ascribed to the A_{1g} and low frequency rigid mode of hexagonal ZnIn₂S₄, respectively.⁴ The observed peaks are in accordance with earlier literature reports.⁴ After formation of BS/BO composite by surface reaction, the intensities of the Raman bands of BO phase are found to decrease significantly. The 123 cm⁻¹ peak of β -Bi₂O₃ is retained in the BS/BO sample along with the appearance of new broad Raman features at 140, 429 and 965 cm⁻¹ which are attributed to Bi-S stretching of Bi₂S₃ species. All the Raman bands due to BS/BO sample are present in case of ternary BZ20BO sample. However, no assignable peak due to ZnIn₂S₄ could be noticed in the ternary sample which may be due to the low crystalline character, alteration in symmetry and change in microstructural property caused by close microscopic contact between the constituent phases.

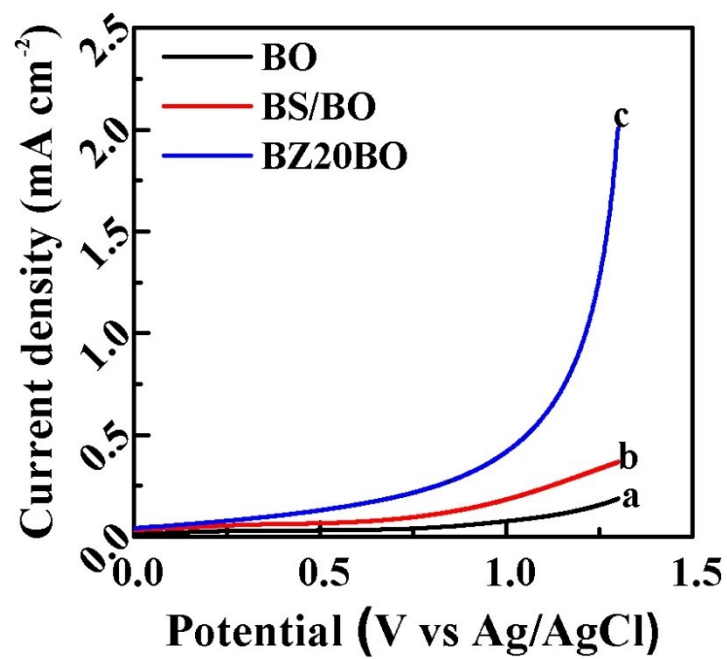


Fig. S9 LSV plots for (a) BO, (b) BS/BO and (c) BZ20BO samples.

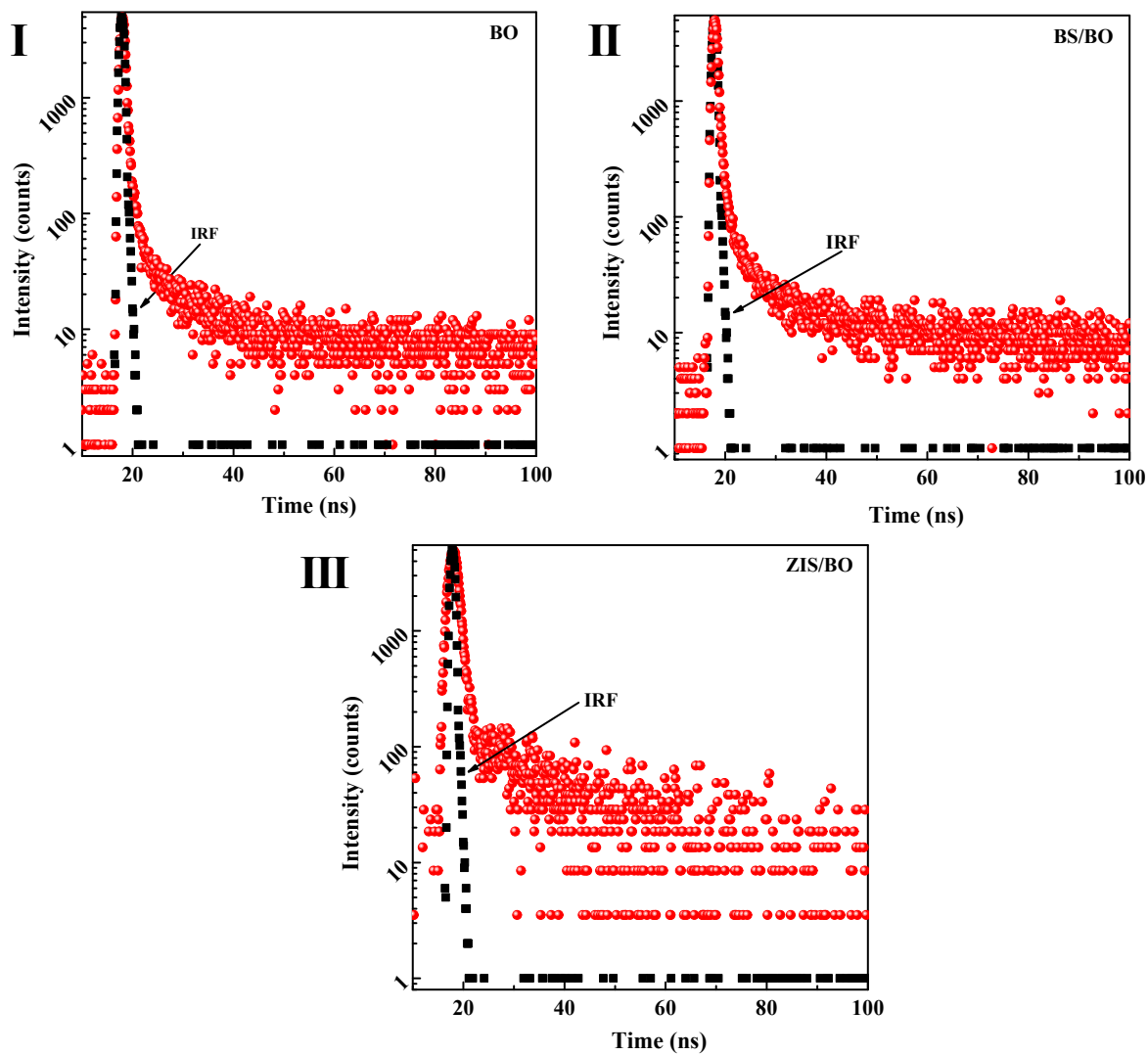


Fig. S10 Time-resolved fluorescence decay for (I) BO, (II) BS/BO and (III) ZIS/BO materials.

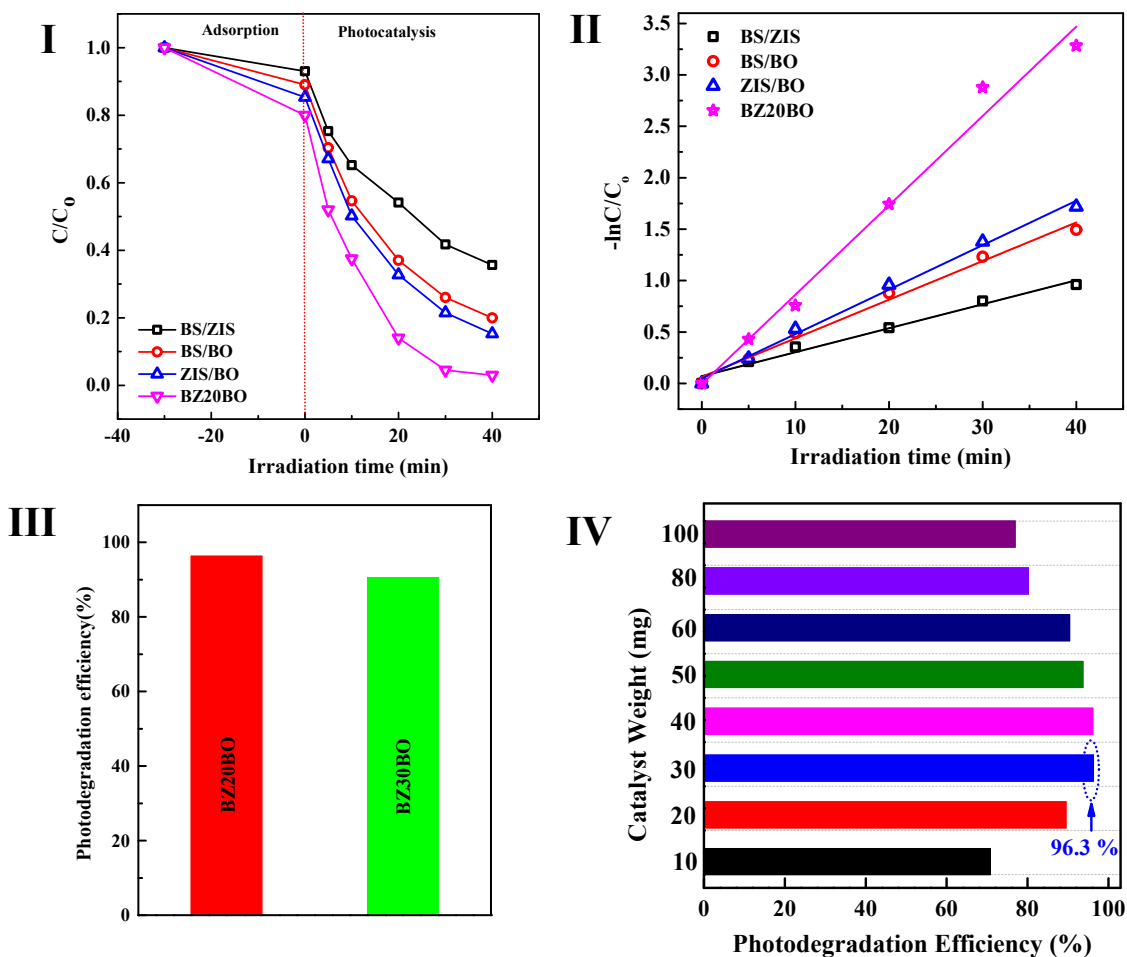


Fig. S11 (I) Photocatalytic degradation of TCN and (II) Pseudo first order kinetic plots for BS/ZIS, BS/BO, ZIS/BO and BZ20BO composite materials, (III) PDE comparison of BZ20BO and BZ30BO samples after 40 min of irradiation time and (IV) Weight variation of BZ20BO photocatalyst for degradation of 20 ppm TCN solution (100 ml).

Effect of Reaction Parameters for TCN Photodegradation.

Optimization of Catalyst Weight and TCN concentration. The photocatalytic experiments for TCN degradation is optimized by varying the catalyst weight between 100-1000 mg/L and TCN concentration in the range of 20-60 ppm. The % photodegradation efficiency (PDE) of TCN using different amount of ternary BZ20BO photocatalyst is represented in Fig. S11IV. Optimized PDE is obtained by using 300 mg/L of the ternary photocatalytic material. Further increase in photocatalyst weight leads to decrease in the PDE which may be due to the scattering of light and aggregation of photocatalyst particles. Further the TCN concentration variation plot presented in Fig. 5III reveals that 20 ppm TCN solution can be efficiently degraded achieving 96.3 % PDE at

optimized catalyst weight of 300 mg/L. A decrease in PDE is observed by increasing the TCN concentration beyond 20 ppm possibly due to the availability of insufficient numbers of surface active sites of BZ20BO material.⁵ An optimized catalyst weight of 30 mg and 20 ppm TCN solution is used for further photocatalytic experiments.

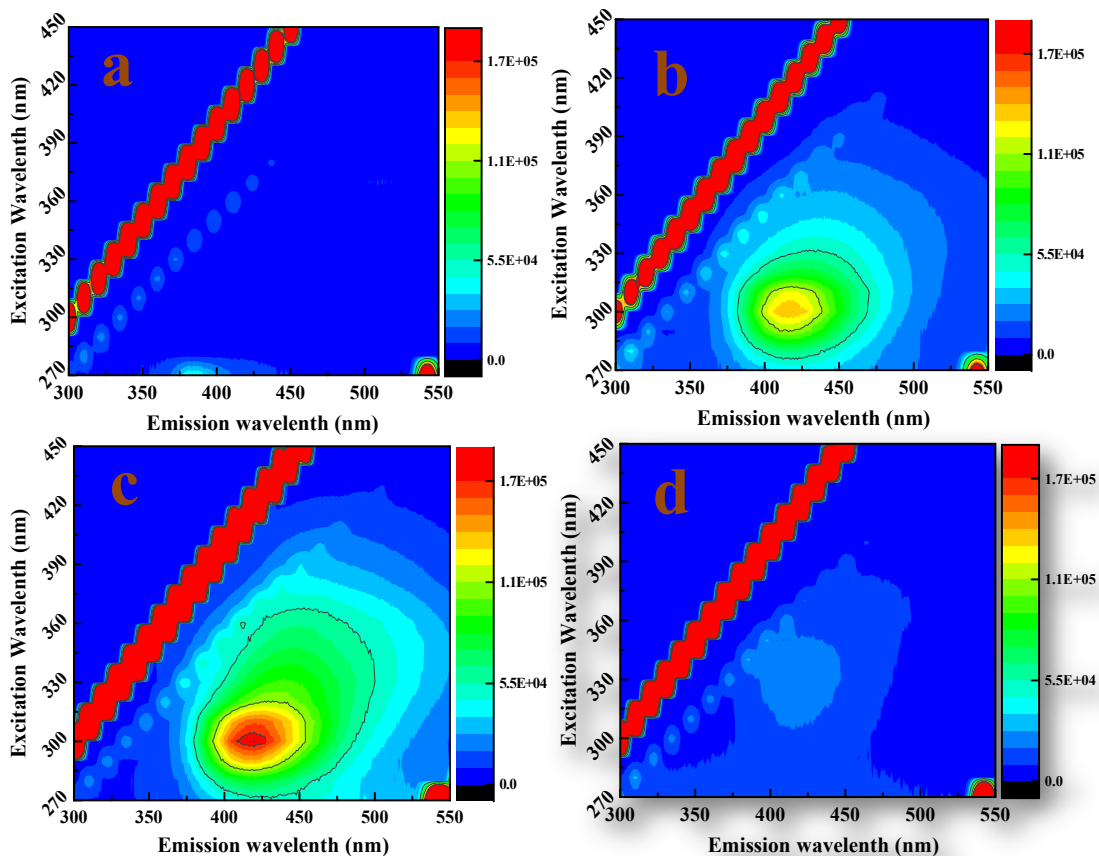


Fig. S12 PL excitation-emission spectra of (a) parent 20 ppm TCN solution and (b-d) TCN solution after irradiation time of 10, 20 and 40 min in presence of BZ20BO photocatalyst.

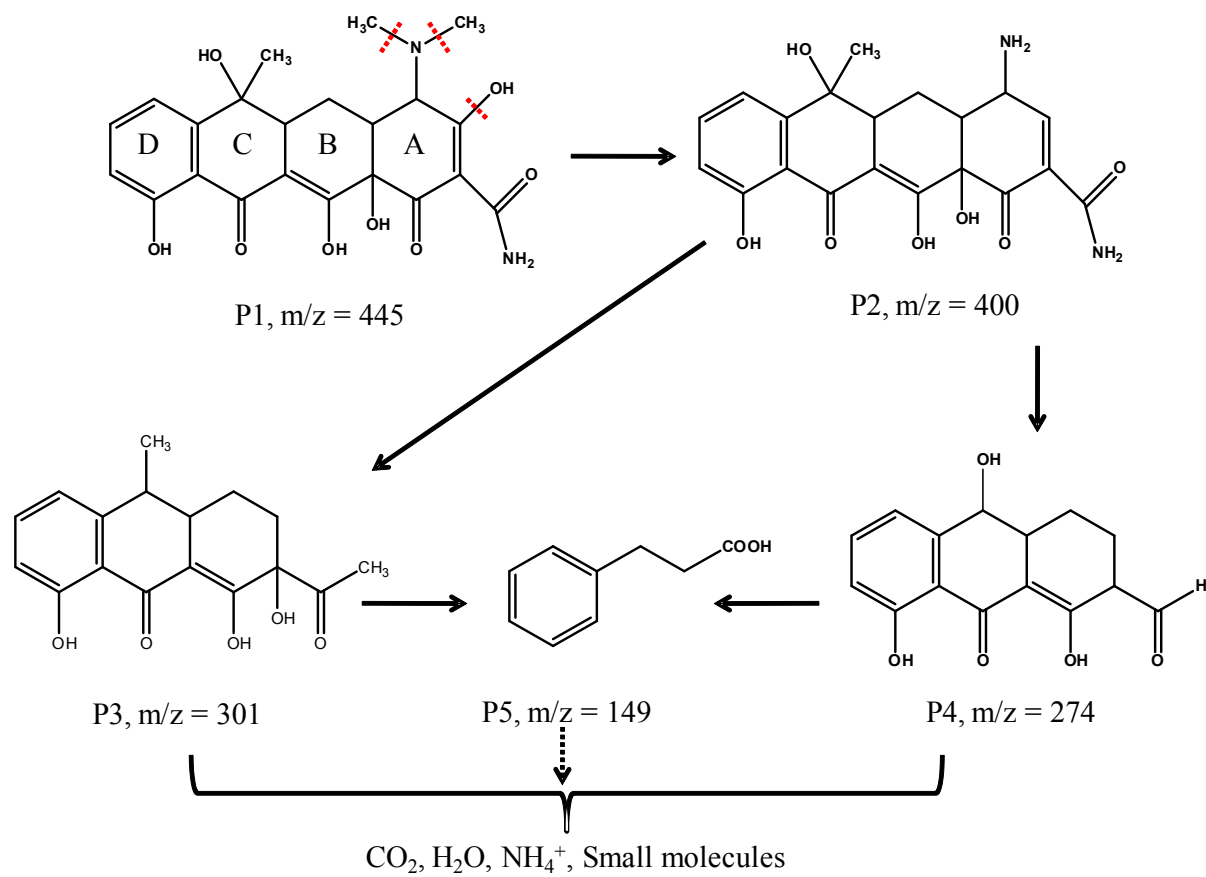


Fig. S13 Degradation pathway of TCN over BZ20BO photocatalyst surface.

The degradation of TCN over BZ20BO photocatalyst is studied by analyzing the reaction mixture at different interval of time using LC-ESI-MS technique. Four aromatic intermediates namely P2, P3, P4 and P5 are detected along with molecular ion peak (P1) of tetracycline at m/z value of 445. Based on the observed intermediates, a plausible degradation pathway for TCN is proposed in Fig. S13. The intermediate product P2 (m/z=400) is formed by loss of both N-methyl groups and a hydroxyl group from P1.⁶ Product P2 undergo breakage of ring A and dehydroxylation reaction by oxidation with the $\bullet\text{OH}$ radicals to give product P3 (m/z = 301). Product P4 (m/z=274) is formed by the degradation of P2 via dislodging of amino groups due to breakage of ring A and a loss of methyl group from ring C.⁷ Product P2 and P4 has been identified earlier as major reaction intermediates during the photocatalytic degradation of tetracycline.⁶⁻⁸ Then product P5 (m/z=149) can be formed through cleavage of ring B, formation of carboxyl group by oxidation and dislodging of hydroxyl groups from product P4. The product P5 can also be formed by

decomposition of P3 in a similar fashion. Finally, product P3, P4 and P5 undergo complete mineralization over BZ20BO photocatalyst to give CO₂, H₂O, and small aliphatic molecules.

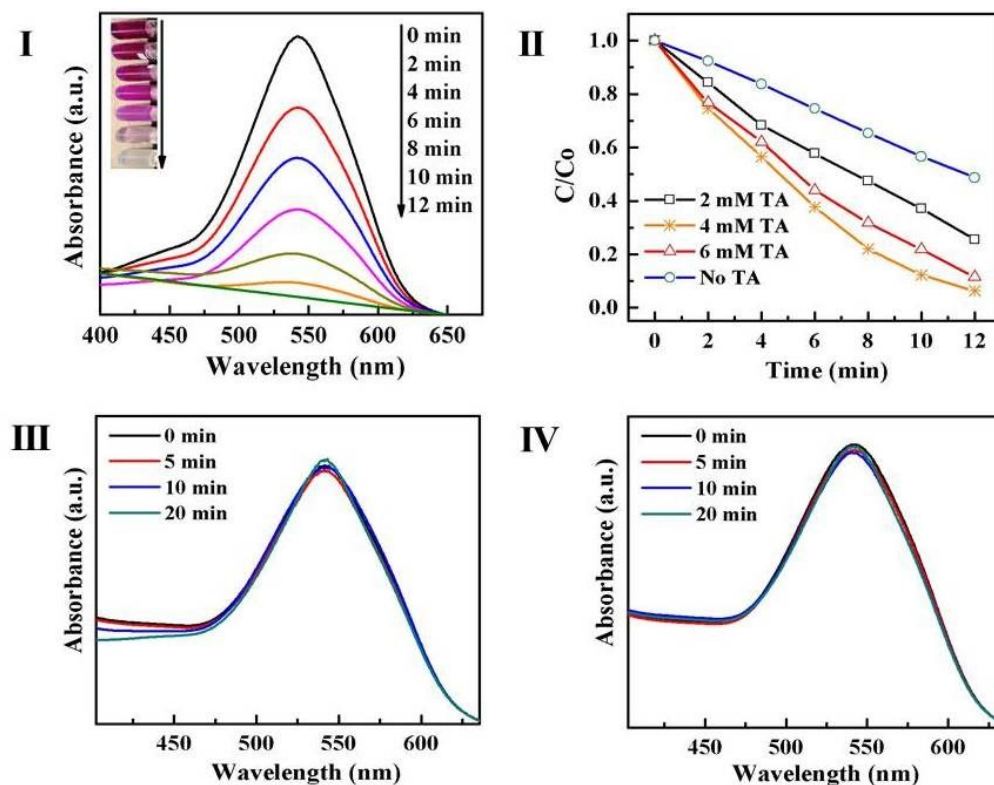


Fig. S14 (I) Change in absorption profile of Cr(VI) in presence of BZ20BO catalyst and 4 mM TA under illuminated condition, (II) effect of different concentration of TA on photocatalytic reduction efficiency of BZ20BO and (III) and (IV) absorbance of Cr(VI) in presence of TA (without catalyst) under dark and illuminated conditions, respectively (the absorption spectra were recorded using diphenylcarbazide as complexing agent).

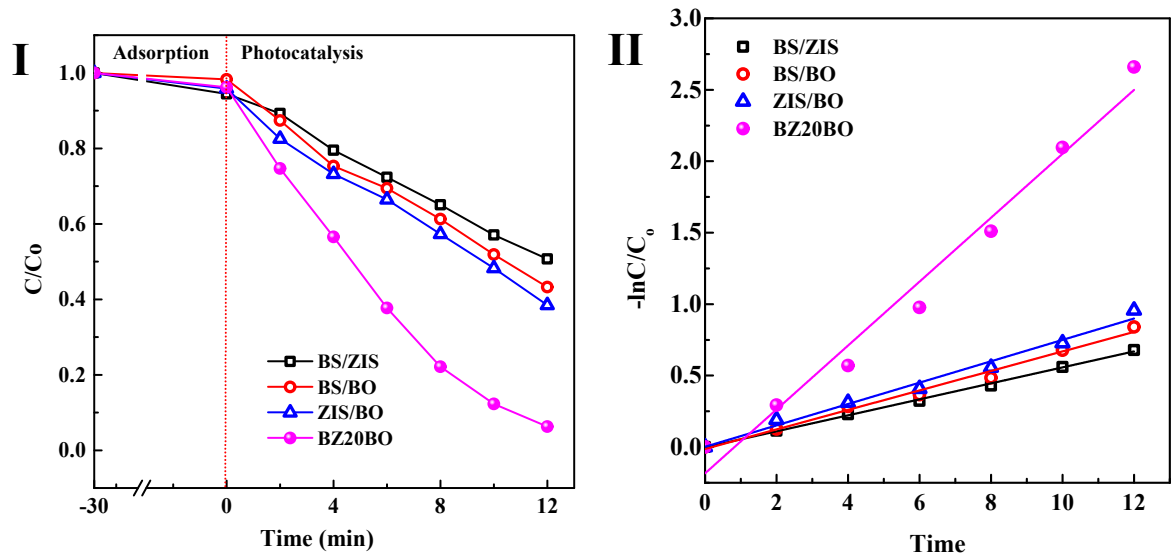


Fig. S15 (I) Comparison of photoreduction efficiency for Cr(VI) and (II) Pseudo first order kinetic plots for BS/ZIS, BS/BO, ZIS/BO and BZ20BO materials.

Calculation of apparent conversion efficiency for H₂ production.⁵

$$\text{Apparent Conversion efficiency (\%)} = \frac{\text{Stored Chemical Energy (SCE)}}{\text{energy of incident light (EIL)}} \times 100$$

$$\text{Stored Chemical Energy (SCE)} = \frac{N(H_2)}{t} \Delta H_C$$

$$= \text{Moles of } H_2 \text{ produced per second} \times \Delta H_C$$

Where $N(H_2)$ = moles of H₂ produced during the reaction,

t = duration of the reaction (sec) and ΔH_C = combustion heat of H₂ (kJ/mol)

$$= 0.623 \mu\text{molsec}^{-1} \times 285.8 \text{ kJ/mol}$$

$$= 0.178 \text{ J/sec}$$

$$\text{Incident light intensity (ILI)} = \frac{Q_i}{4\pi r^2}$$

$$= \frac{250 \text{ W}}{4 \times 3.141 \times (4)^2} = 1.243 \text{ W/cm}^2$$

$Q_i = 250 \text{ W}$, $r = 4 \text{ cm}$ (distance between reactor surface and lamp)

$$\text{Apparent Conversion efficiency (\%)} = \frac{0.178 \text{ J/sec}}{1.243 \text{ W/cm}^2} \times 100$$

$$= 14.3 \%$$

Active Species Trapping Experiments. Scavenger Experiments. In order to verify the role of active radical species responsible for photocatalytic degradation of TCN, scavenger experiments were performed. Typically, different scavengers such as ammonium oxalate (AO), benzoquinone (BQ), AgNO₃ and tertiary butyl hydroxide (t-BuOH) are used to trap hole (h⁺), superoxide (O₂^{•-}), electron (e⁻) and hydroxyl radical (•OH), respectively. The experimental procedures were similar

to photocatalytic experiment for degradation of TCN except the addition of aforementioned scavengers.

Further for deep investigation of the formation of $\cdot\text{OH}$ radicals in the aqueous catalyst suspension, terephthalic acid photoluminescence (TA-PL) probing technique and ESR technique (DMPO used as spin trapping agent) were used. The Nitrobluetetrazolium chloride (NBT) tests and ESR study in methanol suspension of the ternary photocatalyst were performed to confirm the formation of $\cdot\text{O}_2^-$ radicals. All the experiments were carried out using 250 W Xe-lamp as visible light source.

TA-PL Experiment. In a typical experiment, 30 mg of BZ20BO photocatalyst is dispersed in 100 ml of 5×10^{-4} mol/L terephthalic acid solution with the addition of small amount of base until terephthalic acid is dissolved. The whole suspension is placed under illuminated condition for 90 min. At a regular time interval, 3 ml of aliquot was taken out and centrifuged at 3500 rpm to eliminate the catalyst. The resulting supernatant was analyzed using PL technique to measure the rate of formation of fluorescent 2-hydroxy terephthalic acid.

ESR Study. DMPO (5,5'-dimethyl-1-pyrroline-N-oxide) was employed as a spin trapping reagent to trap the $\cdot\text{OH}$ and $\text{O}_2\cdot^-$ radicals in the aqueous and methanol suspension of BZ20BO photocatalyst, respectively. The ESR study was performed according to the literature reported procedure.⁹

Nitrobluetetrazolium Chloride (NBT) Test. In this experiment, 30 mg of BZ20BO photocatalyst was dispersed in 100 ml of 5×10^{-5} mol/L NBT solution and subjected to illumination for 90 min. In a regular time interval, 3 ml of aliquot was taken out and centrifuged at 3500 rpm to separate the dispersed catalyst. The supernatant was analyzed through UV-Vis absorbance spectroscopy to measure the rate of formation of formazan derivatives.

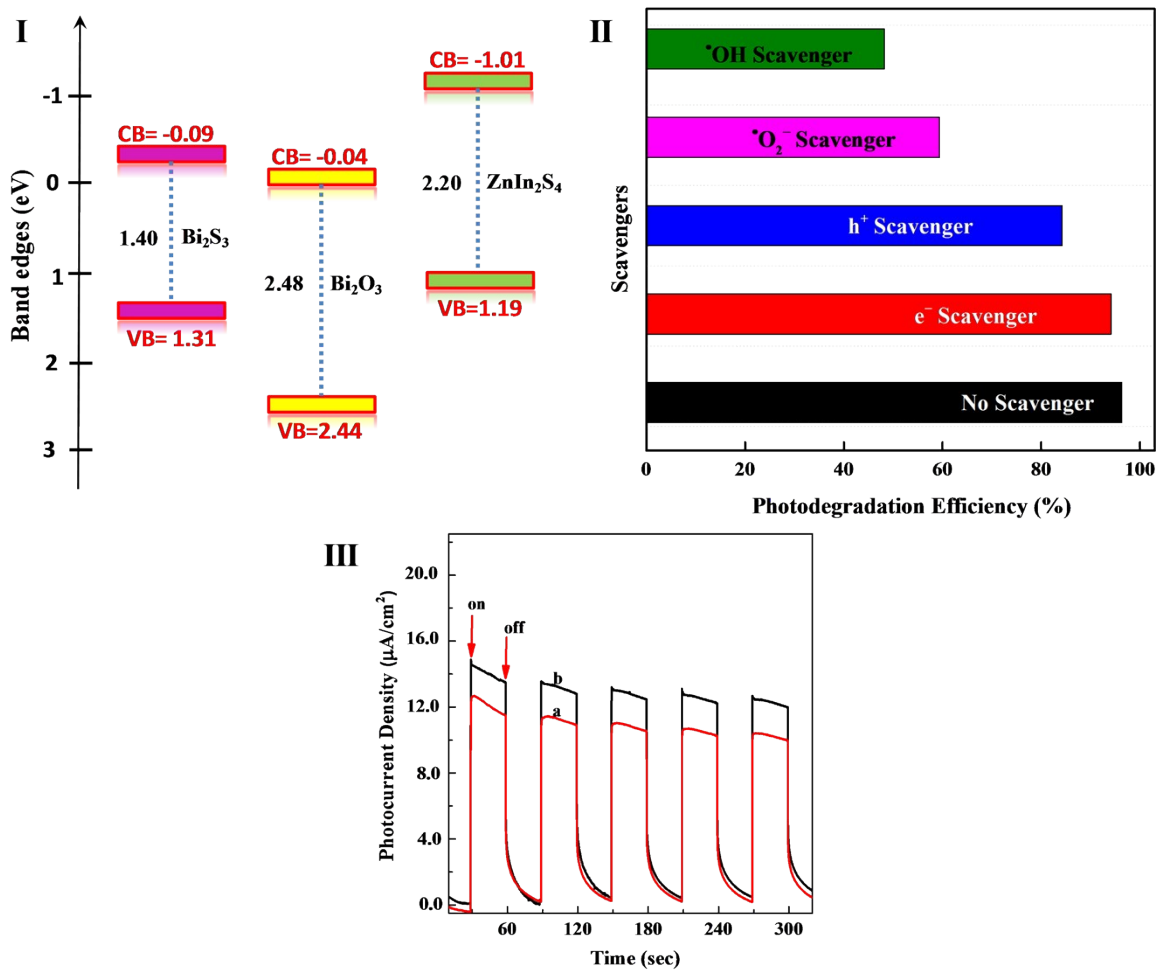


Fig. S16 (I) Band positions of bare semiconductors w.r.t. NHE, **(II)** PDE of BZ20BO photocatalyst for TCN degradation in presence of different radical scavengers and **(III)** Transient photocurrent measurement for BZ20BO photocatalyst (a) in absence and (b) in presence of 20 ppm TCN (0.1 M Na₂SO₄ is used as supporting electrolyte).

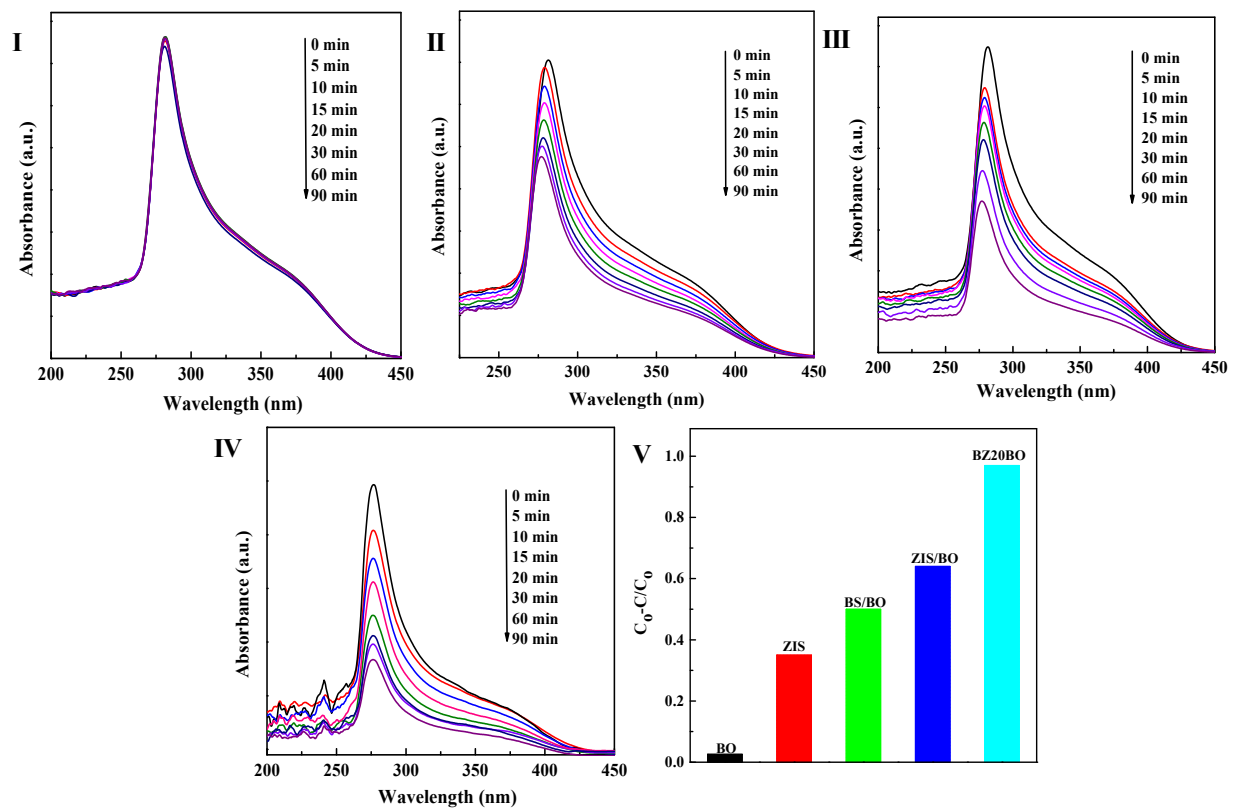


Fig. S17 UV-Vis absorbance spectra of 5×10^{-5} molar nitrobluetetrazolium aqueous solution containing 300 mg/l of (I) BO, (II) ZIS, (III) BS/BO, (IV) ZIS/BO photocatalyst and (V) transformation rate of NBT for different photocatalyst after 30 min of visible light irradiation.

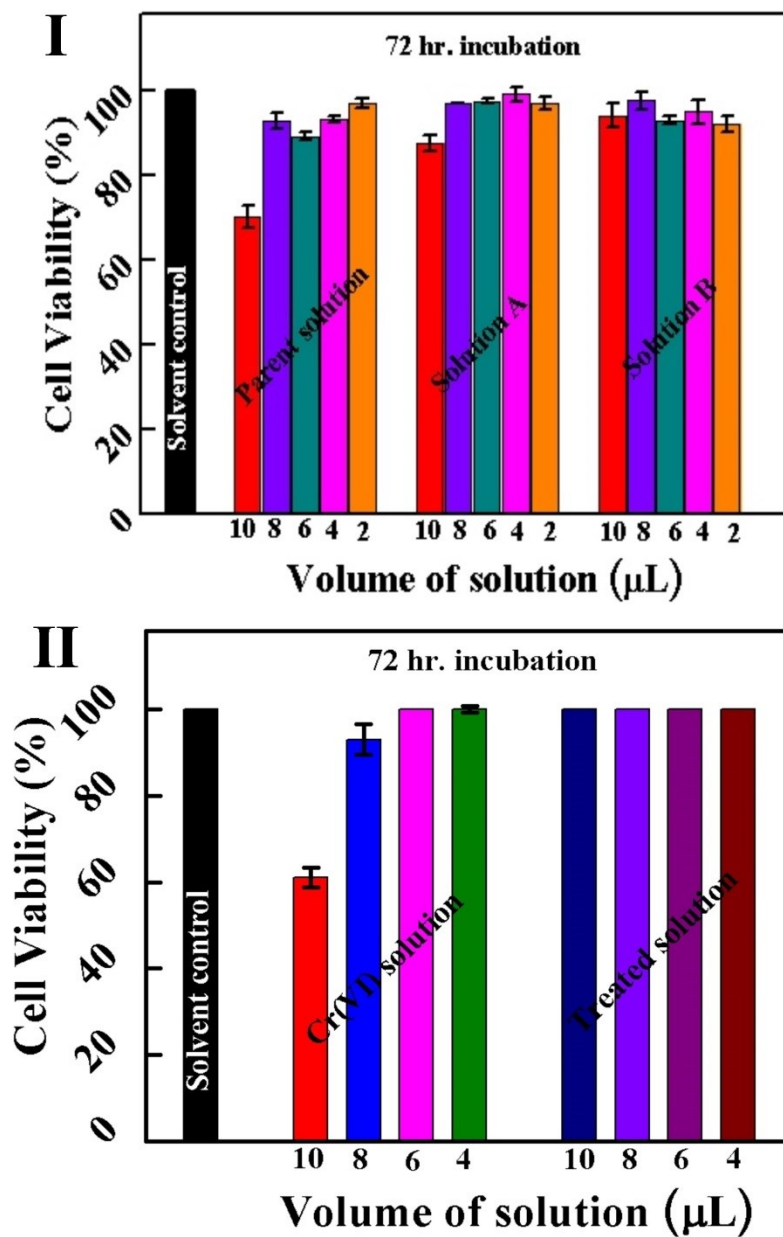


Fig. S18 (I) Cytotoxicity analysis for different volume of aqueous samples collected after 20 min (Solution A) and 40 min (Solution B) of photocatalytic TCN degradation and (II) Cytotoxicity analysis of parent Cr(VI) solution and photocatalytically treated solution.

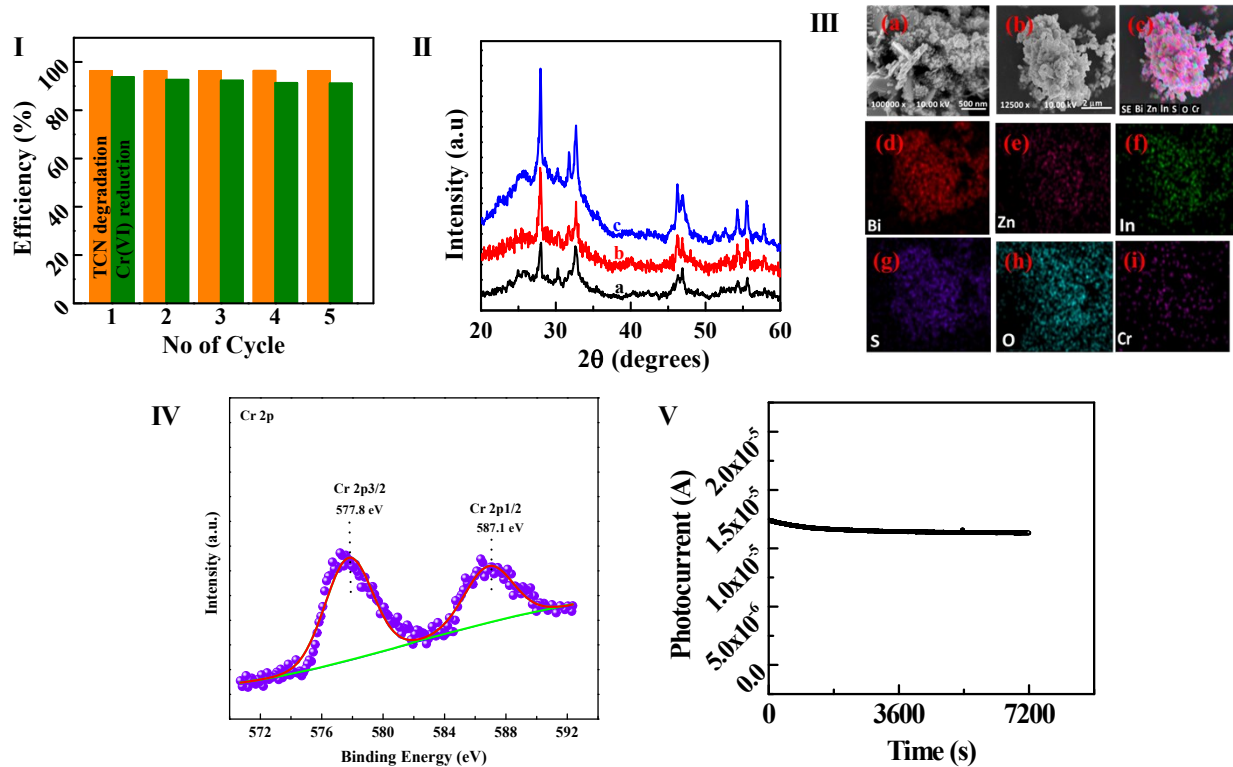


Fig. S19 (I) Recyclability study, (II) XRD patterns of (a) fresh, (b) and (c) after 5th catalytic run of BZ20BO for TCN degradation and Cr(VI) reduction, respectively, (III) FESEM images of reused BS20BO material after (a) TCN degradation and (b) Cr(VI) reduction, (c-h) elemental mapping study of BS20BO material after Cr(VI) reduction (IV) High resolution XPS spectra of Cr species adsorbed on the surface of BS20BO material after photocatalytic reduction of Cr(VI) and (II) long term photo-stability study of BS20BO composite material.

References

1. D. Majhi, P.K. Samal, K. Das, S.K. Gouda, Y.P. Bhoi, B.G. Mishra, *ACS Appl. Nano Mater.*, 2019, **2**, 395–407.
2. R.A. Geioushy, S.M. El-Sheikh, A.B. Azzam, B.A. Salah, F.M. El-Dars, *J. Hazard. Mater.*, 2020, **381**, 120955.
3. W. Wang, Y. Yu, T. An, G. Li, H.Y. Yip, J.C. Yu, P.K. Wong, *Environ. Sci. Technol.*, 2012, **46**, 4599–4606.
4. S. Shen, L. Zhao, X. Guan, L. Guo, *J. Phys. Chem. Solids*, 2012, **73**, 79–83.
5. R. Bariki, D. Majhi, K. Das, A. Behera, B.G. Mishra, *Appl. Catal., B.*, 2020, **270**, 118882.
6. J.F. Niu, S.Y. Ding, L.W. Zhang, J.B. Zhao, C.H. Feng, *Chemosphere* 2013, **93**, 1–8.
7. X.L. Liu, P. Lv, G.X. Yao, C.C. Ma, P.W. Huo, Y.S. Yan, *Chem. Eng. J.*, 2013, **217**, 398–406.
8. M. Cao, P. Wang, Y. Ao, C. Wang, J. Hou, J. Qian, *J. Colloid Interface Sci.* 2016, **467**, 129–139.
9. X. Xu, Y. Sun, Z. Fan, D. Zhao, S. Xiong, B. Zhang, S. Zhou, G. Liu, *Front. Chem.*, doi: 10.3389/fchem.2018.00064.